A real-time ARMS PCR/high-resolution melt curve assay for the detection of the three primary mitochondrial mutations in Leber's hereditary optic neuropathy

Siobhan Eustace Ryan,[1] Fergus Ryan,[2] Veronica O'Dwyer,[1] Derek Neylan[2]

[1]National Optometry Centre, Dublin Institute of Technology, Dublin, Ireland; [2]School of Biological Sciences, Dublin Institute of Technology, Dublin, Ireland

Purpose: Approximately 95% of patients who are diagnosed with Leber's hereditary optic neuropathy (LHON) have one of three mitochondrial point mutations responsible for the disease, G3460A, G11778A, and T14484C. The purpose of this study was to develop a novel multiplex real-time amplification-refractory mutation system (ARMS) PCR combined with high-resolution melt curves to identify the individual mutations involved. The study aimed to provide a more robust, cost- and time-effective mutation detection strategy than that offered with currently available methods. The assay reported in this study will allow diagnostic laboratories to avoid costly next-generation sequencing (NGS) assays for most patients with LHON and to focus resources on patients with unknown mutations that require further analysis.
Methods: The test uses a combination of multiplex allele-specific PCR (ARMS PCR) in combination with a high-resolution melt curve analysis to detect the presence of the mutations in G3460A, G11778A, and T14484C. PCR primer sets were designed to produce a control PCR product and PCR products only in the presence of the mutations in 3460A, 11778A, and 14484C in a multiplex single tube format. Products produce discrete well-separated melt curves to clearly detect the mutations.
Results: This novel real-time ARMS PCR/high-resolution melt curve assay accurately detected 95% of the mutations that cause LHON. The test has proved to be robust, cost- and time-effective with the real-time closed tube system taking approximately 1 h to complete.
Conclusions: A novel real-time ARMS PCR/high-resolution melt curve assay is described for the detection of the three primary mitochondrial mutations in LHON. This test provides a simple, robust, easy-to-read output that is cost- and time-effective, thus providing an alternative method to individual endpoint PCR-restriction fragment length polymorphism (RFLP), PCR followed by Sanger sequencing or pyrosequencing, and next-generation sequencing.

Leber's hereditary optic neuropathy (LHON; OMIM 535000) is an inherited neuropathy caused by primary mtDNA mutations leading to bilateral optic atrophy [1,2]. As a result, visual prognosis is poor with the majority of patients with LHON registered as legally blind. This profound loss of vision in affected subjects is due to the targeted destruction of the highly specialized retinal ganglion cells (RGCs) [3]. Patients with LHON usually present initially with painless, subacute loss of vision in one eye, with the second eye becoming affected in the following weeks to months.

LHON has a prevalence of 1 in 31,000 in northern England, 1 in 39,000 in the Netherlands, and 1 in 50,000 in Finland [4-6]. The disease typically affects a young demographic, with peak onset between the ages of 15 and 30 years [7]. Patient carriers of LHON mutations who have not experienced any loss of vision before age 50 are likely not to do so.

However, several patients with LHON have suffered visual failure from as young as 2 years and as old as 87 years of age [8]. LHON demonstrates distinctive clinical signs, such as incomplete penetrance and an obvious gender bias with approximately 50% of male carriers and only 10% of female carriers developing the disease [9], suggesting that other genetic factors and/or the environment must play a role in disease penetrance [10-12].

Approximately 95% of those diagnosed with LHON have one of three primary mitochondrial mutations affecting complex I subunits of the respiratory chain—G3460A (A52T of ND1), G11778A (R340H of ND4), and T14484C (M64V of ND6) [13-15]—while other rare mutations (such as G13730A, G14459A, C14482G, A14495G, C14498T, C14568T, and T14596A) account for the final 5% [16-23]. LHON specifically targets the RGCs that are highly susceptible to oxidative stress and mitochondrial dysfunction [3]. Interestingly, some visual recovery can occur in patients with LHON, but the extent of this recovery is dependent upon the mutation involved in that patient's LHON. The point mutation T14484C exhibits some visual recovery in (58%) of patients

Correspondence to: Siobhan Eustace Ryan, National Optometry Centre, Dublin Institute of Technology, Kevin Street, Dublin 8, Ireland; Phone: 353 1 4024900, FAX: 353 1 4024915; email: siobhan.eustace@dit.ie

with LHON, followed by the point mutation G3460A at 25%. Patients who harbour the G11778A mutation have the lowest level of visual recovery [24-27].

Current diagnostic strategies for the three most common mutations that cause LHON include individual endpoint PCR-restriction fragment length polymorphism (RFLP) [28], multiplex PCR-RFLP [29], allele-specific PCR [30], real-time PCR [31], and PCR followed by Sanger sequencing or pyrosequencing [32]. A targeted next-generation sequencing (NGS) panel is available for mitochondrial sequencing (mtSEEK®), and open source bioinformatics software is also available for extracting mitochondrial sequences from NGS exome sequences [33]. This study aimed to develop a novel multiplex closed tube real-time assay to detect the three common mutations using a combination of allele-specific amplification and high-resolution melt curve analysis. The assay will allow diagnostic laboratories to avoid costly NGS for most LHON cases.

METHODS

Patient DNAs were obtained from the Centre for Medical Genetics, Our Lady's Hospital for Sick Children, Dublin, Ireland and Oxford Medical Genetics Laboratories, Oxford, UK. Subjects gave written consent for the testing of their DNA for the 3 primary mutations causing LHON. All subject samples used in this study were previously tested for the 3 primary mutations using simplex PCR and bidirectional DNA sequencing and the results reported. To maintain patient confidentiality, aliquots of residual DNA material from the diagnostic test were labelled with the LHON mutation detected and irreversibly anonymised. The use of subject DNA in this study has received ethical approval from the Dublin Institute of Technology Research Ethics Committee. This study adhered to the tenets of the Declaration of Helsinki and the ARVO statement on human subjects.

PCR primer sets (Sigma Genosys, Arklow, Ireland, Table 1) were designed to produce PCR products only in the presence of the 3460A, 11778A, and 14484C mutations and not in the presence of any of the wild-type sequences. The positions of the primers are highlighted in the complete mitochondrial genome (NCBI Reference Sequence; NC_012920.1) in Appendix 1. To control for DNA quality and PCR conditions, a control primer set was included that amplifies genomic insulin sequences (Table 1 and Appendix 2, NCBI Sequence: E00022.1). To clearly differentiate the control and mutation-specific PCR products in a multiplex melt curve analysis, the thermodynamic stability (melting temperature) of the PCR products was initially estimated using uMELT [34] software before experimental analysis in a single tube. All double-stranded DNA sequences have the property that the temperature at which they become single stranded is determined by the sequence composition and the length of the DNA sequence [35]. Several different PCR products can thus be differentiated in a mixture, if the products each have different melting temperatures. The insulin control primer set (INS F/R) was chosen because of its own distinct melting point compared to the three mutations under investigation. A β-globin control primer set was also evaluated but not considered as the melting temperature was not easily distinguishable from that of the LHON mutations.

Simplex PCR for the determination of melting temperatures of individual PCR products was performed on an

TABLE 1. PCR PRIMERS USED IN THE DIAGNOSTIC TEST.			
Mutation	**Primer (5'-3')**	**Product size (Position)**	**Melt temperature average (range)**
3460**A** ARMS	F: TACTACAACCCTTCGCTGcC**A***	120 bp (3440–3559)	82.58 °C (82.32 - 83.14)
	R: GTAGAAGAGCGATGGTGAGAGCTAAG		
11778**A** ARMS	F: ACGAACGCACTCACAGTg**A**	143 bp (11,760-11902)	80.32 °C (80.08 - 80.7)
	R: CACAGAGAGTTCTCCCAGTAGGTTAA		
14484**C** ARMS	F: GTAGTATATCCAAAGACAACgA**C***	161 bp (14,462-14622)	76.31 °C (76.01 - 76.77)
	R: GGGTTTTCTTCTAAGCCTTCTCC		
Insulin control	F: GACTGAATTCCGGCACGTCCTGGCAGTG	221 bp (1458–1658)	90.24 °C (90.04 - 90.68)
	R: GACTCTCGAGGGAGGCGGCGGGTGTG		

The bases highlighted in bold result in allele specific amplification of the 3460A, 11778A and 14484C mutated sequences respectively. Lower case bases highlight mismatches to increase the specificity of the allele specific amplification. The PCR product sizes, positions in Homo sapiens mitochondrion, complete genome (NCBI Reference Sequence: NC_012920.1) or genomic insulin sequence (E00022.1) and average melting temperatures are highlighted. The melting temperatures are based on at least 9 separate experiments. The 2 primers marked with * have previously been published by Bi et al. 2010 [30].

ABI 7500 Fast (Life Technologies, Carlsbad, CA) real-time PCR instrument in a reaction containing 50 ng of genomic DNA, 100 ng of the appropriate primer mix, and 7.5 µl of PowerUp SYBR Green Master Mix (Life Technologies) in a total volume of 15 µl. The PCR conditions were 95 °C for 2 min, followed by 35 cycles of 95 °C for 3 s, and 60.5 °C for 30 s. This was followed by melt curve analysis at 95 °C for 15 s, 60 °C for 1 min, and continuous detection up to 95 °C. For multiplex analysis, these cycling conditions were used on 50 ng of DNA and a primer mix containing 20 ng of 3460 amplification-refractory mutation system (ARMS) F/R, 35 ng of 11,778 ARMS F/R, 250 ng of 14,484 ARMS F/R, and 15 ng of INS F/R. During optimization of the protocol, products were also detected with electrophoresis on a 2.5% agarose gel (Life Technologies) containing 0.5 µg/ml ethidium bromide (catalogue no. E7637; Sigma Genosys, Arklow, Ireland).

RESULTS

The test is designed such that the control sequence will always produce a product, while the presence of one of the mutations will be detected by the additional amplification of the corresponding allele-specific PCR product. The presence of the control PCR product in the absence of any of the mutation-specific PCR products indicates the absence of the three mutations. The presence of the control product in the presence of one of the mutation-specific PCR products indicates the presence of the mutation. The resultant PCR products can be visualized (if required) on an ethidium bromide–stained agarose gel (Figure 1A), but the SYBR green dye and melting curves detect and differentiate the control and allele-specific products in real time. The melting temperatures of the 3460A, 11778A, 14484C, β–globin, and INS control products were 82.58 °C, 80.32 °C, 76.31 °C, 86.03 °C, and 90.24 °C, respectively, allowing clear differentiation of the allele-specific products as shown in Figure 1B. As the melting temperature of the INS product is significantly different from any of the
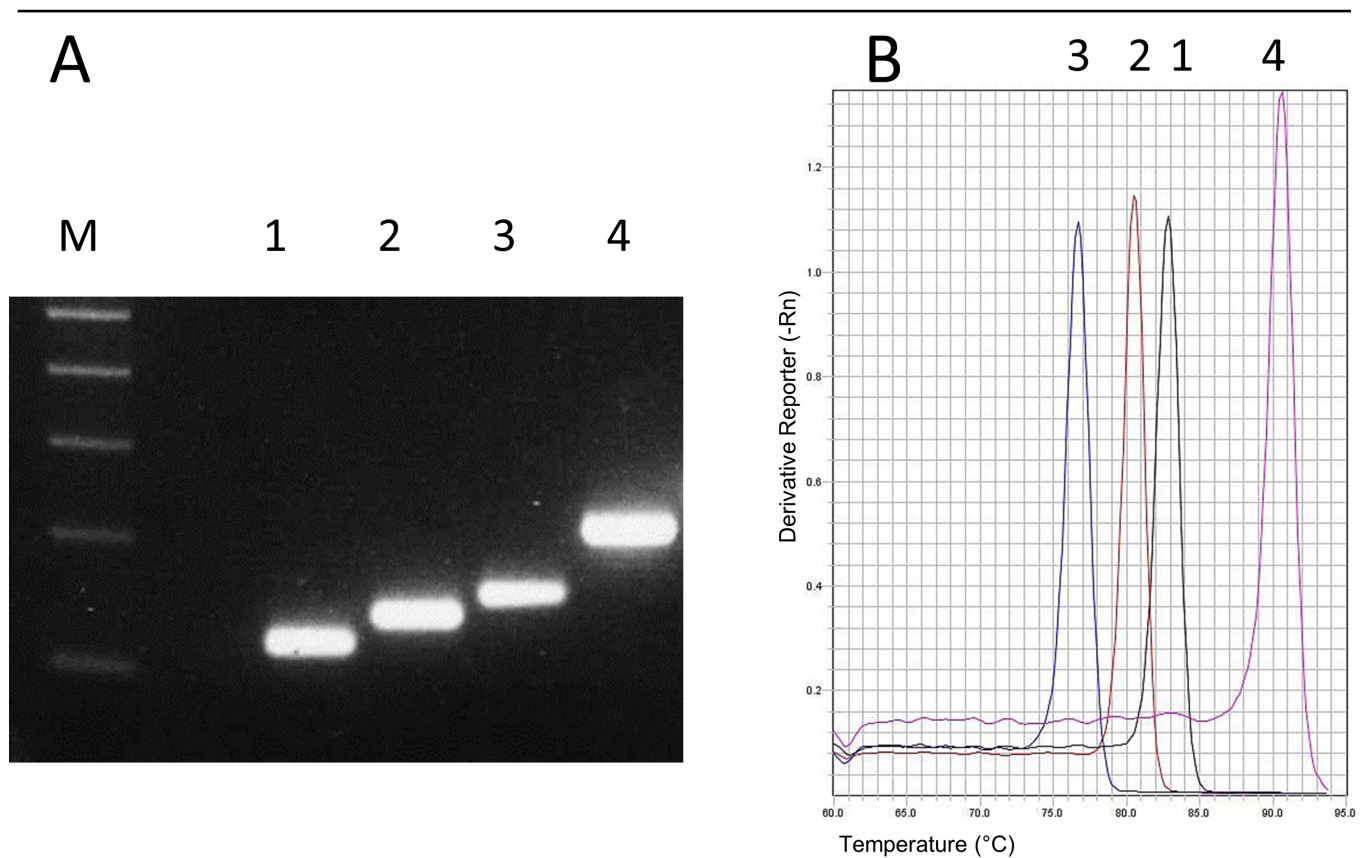

Figure 1. Melt temperatures of individual PCR products. **A**: 2.5% ethidium bromide stained agarose gel showing the results of simplex PCR amplification of 3460A, 1177A, and 14484C allele–specific products and insulin and control product (1, 2, 3, 4, respectively). **B**: Melt curve generated on ABI 7500 Fast of the same products demonstrating the different melting temperatures of the allele-specific products and the control products. 3460A, 82.58 °C; 11778A, 80.32 °C; 14484C, 76.31 °C; INS, 90.24 °C.
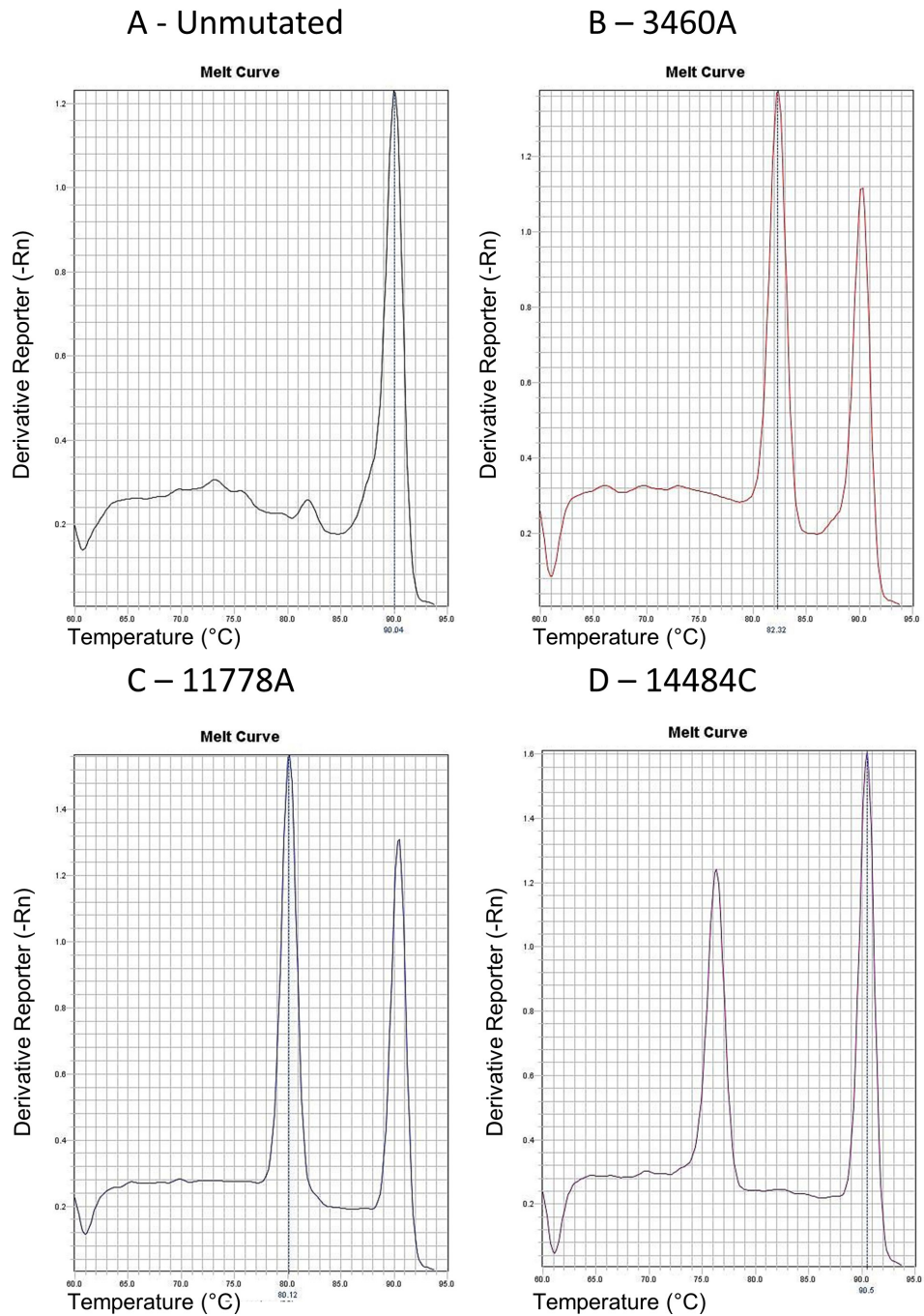
A - Unmutated

B – 3460A

C – 11778A

D – 14484C

Figure 2. Multiplex real-time analysis of LHON subject samples. **A**: Unmutated DNA; only the control product is amplified. **B**: Subject DNA with mutation in 3460A; products at 90.04 °C and 82.32 °C. **C**: Subject DNA with mutation in 11778A; products at 90.04 °C and 80.12 °C. **D**: Subject DNA with mutation in 14484C mutation; products at 90.04 °C and 76.32 °C.

allele-specific products, this product was chosen for the multiplex analysis.

Multiplex analysis using a combination of the three allele-specific primer sets and the INS control primer set provided clear and robust detection of the three mutations in the subject control samples as demonstrated in Figure 2. Figure 3 shows the four samples on a 2.5% agarose gel and on a real-time melt curve screen, demonstrating the clear differentiation of the allele-specific products using melting temperatures.

DISCUSSION AND CONCLUSION

This study aimed to develop a novel ARMS PCR / high resolution melt curve-based multiplex assay for the detection of the three most common mutations leading to LHON. Approximately 95% of patients with LHON have one of the three common mutations, G3460A (13%), G11778A (69%) and T14484C (14%), with other rare mutations accounting for the final 5%. This assay robustly detected the three primary mitochondrial mutations causing LHON in less than 1 h at a cost that is significantly lower than individual PCR-RFLP [28], multiplex PCR-RFLP [29], bidirectional Sanger sequencing or pyrosequencing sequencing [32], and next-generation sequencing methodologies [33]. This assay provides a significant advantage over current technologies.
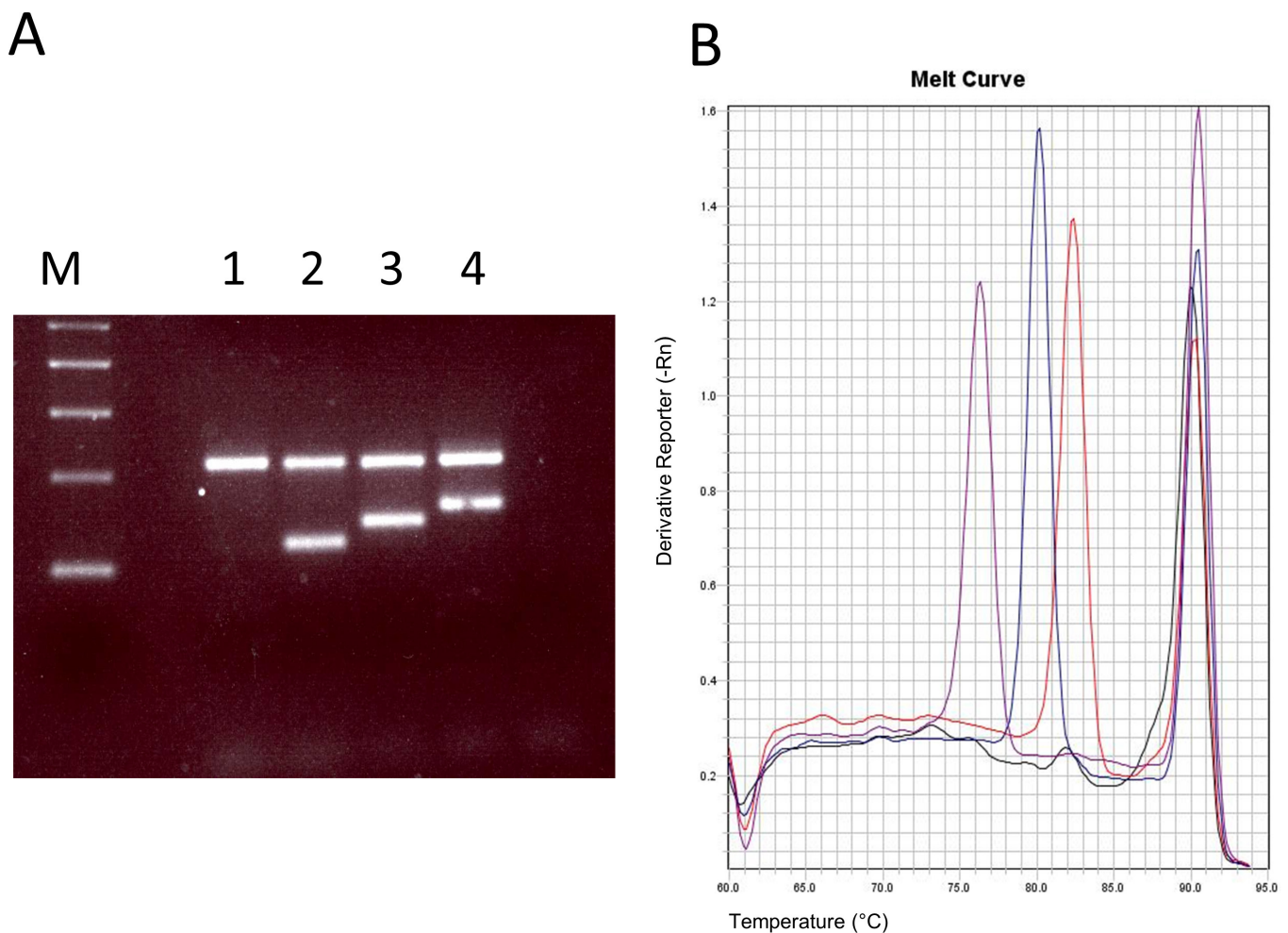

Figure 3. Multiplex Real time ARMS / High resolution melt PCR.. **A**: 2.5% ethidium bromide stained agarose gel showing the results of multiplex PCR amplification of (1) unmutated DNA and (2–4) subject DNA with mutations in 3460A, 1177A, and 14484C. The control 221 bp Ins PCR product is present in all lanes with the allele-specific products appearing only in the 3460A (120 bp), 1177A (143 bp), and 14484C (161 bp) subject samples. **B**: Multiplex real-time melt curves show clear differentiation of the melt peaks for the control (90. 68 °C), 3460A (82.32 °C), 11,778 (80.12 °C), and 14484C (76.32 °C). All samples produce the control products while the presence of a mutation is detected by the additional allele-specific amplification of the mutation-specific products with a melt temperature at the appropriate temperature.

As can be seen in Figure 1 and Figure 2, mutation identification in subjects is clear and robust. This assay could be implemented in any laboratory with a SYBR Green–capable real-time PCR machine and with minimal optimization and setup time. We suggest that the assay described will detect 95% of the mutations that cause LHON at minimal cost with a rapid turnaround time. The genetic testing registry (NCBI; accessed May 2016) shows that most LHON testing involves uni- or bidirectional Sanger sequencing targeted to the three primary mutations (n = 21), targeted simplex PCR-RFLP (n = 7), and other testing methods (including real-time mutation detection, PCR followed by hybridization and pyrosequencing; n = 4) with two laboratories offering a targeted 37 mitochondrial gene NGS panel (mtSEEK®). The assay described in this manuscript would allow many laboratories testing for LHON to rule out the established mutations 3460A, 11778A, and 14484C in 95% of tests, thus focusing NGS resources on the remaining 5% of test samples.

APPENDIX 1.

Reference mitochondrial genome sequence (NC_012920.1) highlighting the positions of ND1, ND4 and ND6 genes in yellow. Also shown are the positions of the G3460A, G11778A and T14484C mutations (arrows) and the positions of the forward and reverse primers used in the study (red). The sequence was retrieved from NCBI and presented using BioEdit. To access the data, click or select the words "Appendix 1."

APPENDIX 2.

Genomic sequence for human pre pro insulin (E00022.1) highlighting the positions the forward and reverse primers used in the study (red). The sequence was retrieved from NCBI and presented using BioEdit. Additional sequences on the 5' end of the primers are used for cloning purposes and contain EcoRI and XhoI restriction sites. To access the data, click or select the words "Appendix 2."

REFERENCES

1. Leber T. Ueber hereditaere und congenital angelegte sehnervenleiden. Graefes Arch Ophthalmol. 1871; 17:249-91. .

2. Sadun AA, La Morgia C, Carelli V. Leber's Hereditary Optic Neuropathy. Curr Treat Options Neurol 2011; 13:109-17. [PMID: 21063922].

3. Saadati HG, Hsu HY, Heller KB, Sadun AA. A histopathologic and morphometric differentiation of nerves in optic nerve hypoplasia and Leber hereditary optic neuropathy. Arch Ophthalmol 1998; 116:911-6. [PMID: 9682705].

4. Man PY, Griffiths PG, Brown DT, Howell N, Turnbull DM, Chinnery PF. The epidemiology of Leber hereditary optic neuropathy in the North East of England. Am J Hum Genet 2003; 72:333-9. [PMID: 12518276].

5. Spruijt L, Kolbach DN, de Coo RF, Plomp AS, Bauer NJ, Smeets HJ, de Die-Smulders CE. Influence of mutation type on clinical expression of Leber hereditary optic neuropathy. Am J Ophthalmol 2006; 141:676-82. [PMID: 16564802].

6. Puomila A, Hamalainen P, Kivioja S, Savontaus ML, Koivumaki S, Huoponen K, Nikoskelainen E. Epidemiology and penetrance of Leber hereditary optic neuropathy in Finland. European journal of human genetics Eur J Hum Genet 2007; 15:1079-89. [PMID: 17406640].

7. Yu-Wai-Man P, Griffiths PG, Hudson G, Chinnery PF. Inherited mitochondrial optic neuropathies. J Med Genet 2009; 46:145-58. [PMID: 19001017].

8. Dimitriadis K, Leonhardt M, Yu-Wai-Man P, Kirkman MA, Korsten A, De Coo IF, Chinnery PF, Klopstock T. Leber's hereditary optic neuropathy with late disease onset: clinical and molecular characteristics of 20 patients. Orphanet J Rare Dis 2014; 9:158-[PMID: 25338955].

9. Harding AE, Sweeney MG, Govan GG, Riordan-Eva P. Pedigree analysis in Leber hereditary optic neuropathy families with a pathogenic mtDNA mutation. Am J Hum Genet 1995; 57:77-86. [PMID: 7611298].

10. Kerrison JB, Miller NR, Hsu F, Beaty TH, Maumenee IH, Smith KH, Savino PJ, Stone EM, Newman NJ. A case-control study of tobacco and alcohol consumption in Leber hereditary optic neuropathy. Am J Ophthalmol 2000; 130:803-12. [PMID: 11124301].

11. Tsao K, Aitken PA, Johns DR. Smoking as an aetiological factor in a pedigree with Leber's hereditary optic neuropathy. Br J Ophthalmol 1999; 83:577-81. [PMID: 10216058].

12. Johns DR, Smith KH, Miller NR, Sulewski ME, Bias WB. Identical twins who are discordant for Leber's hereditary optic neuropathy. Arch Ophthalmol 1993; 111:1491-4. [PMID: 8240103].

13. Wallace DC, Singh G, Lott MT, Hodge JA, Schurr TG, Lezza AM, Elsas LJ 2nd, Nikoskelainen EK. Mitochondrial DNA mutation associated with Leber's hereditary optic neuropathy. Science 1988; 242:1427-30. [PMID: 3201231].

14. Howell N, Bindoff LA, McCullough DA, Kubacka I, Poulton J, Mackey D, Taylor L, Turnbull DM. Leber hereditary optic neuropathy: identification of the same mitochondrial ND1

mutation in six pedigrees. Am J Hum Genet 1991; 49:939-50. [PMID: 1928099].

15. Johns DR, Neufeld MJ, Park RD. An ND-6 mitochondrial DNA mutation associated with Leber hereditary optic neuropathy. Biochem Biophys Res Commun 1992; 187:1551-7. [PMID: 1417830].

16. Howell N, Halvorson S, Burns J, McCullough DA, Paulton J. When does bilateral optic atrophy become Leber hereditary optic neuropathy? Am J Hum Genet 1993; 53:959-63. [PMID: 8213825].

17. Jun AS, Brown MD, Wallace DC. A mitochondrial DNA mutation at nucleotide pair 14459 of the NADH dehydrogenase subunit 6 gene associated with maternally inherited Leber hereditary optic neuropathy and dystonia. Proc Natl Acad Sci USA 1994; 91:6206-10. [PMID: 8016139].

18. Howell N, Bogolin C, Jamieson R, Marenda DR, Mackey DA. mtDNA mutations that cause optic neuropathy: how do we know? Am J Hum Genet 1998; 62:196-202. [PMID: 9443868].

19. Chinnery PF, Brown DT, Andrews RM, Singh-Kler R, Riordan-Eva P, Lindley J, Applegarth DA, Turnbull DM, Howell N. The mitochondrial ND6 gene is a hot spot for mutations that cause Leber's hereditary optic neuropathy. Brain 2001; 124:209-18. .

20. Wissinger B, Besch D, Baumann B, Fauser S, Christ-Adler M, Jurklies B, Zrenner E, Leo-Kottler B. Mutation analysis of the ND6 gene in patients with Lebers hereditary optic neuropathy. Biochem Biophys Res Commun 1997; 234:511-5. [PMID: 9177303].

21. De Vries DD, Went LN, Bruyn GW, Scholte HR, Hofstra RM, Bolhuis PA, van Oost BA. Genetic and biochemical impairment of mitochondrial complex I activity in a family with Leber hereditary optic neuropathy and hereditary spastic dystonia. Am J Hum Genet 1996; 58:703-11. [PMID: 8644732].

22. Liang M, Jiang P, Li F, Zhang J, Ji Y, He Y, Xu M, Zhu J, Meng X, Zhao F, Tong Y, Liu X, Sun Y, Zhou X, Mo JQ, Qu J, Guan MX. Frequency and spectrum of mitochondrial ND6 mutations in 1218 Han Chinese subjects with Leber's hereditary optic neuropathy. Invest Ophthalmol Vis Sci 2014; 55:1321-31. [PMID: 24398099].

23. Jiang P, Liang M, Zhang J, Gao Y, He Z, Yu H, Zhao F, Ji Y, Liu X, Zhang M, Fu Q, Tong Y, Sun Y, Zhou X, Huang T, Qu J, Guan MX. Prevalence of Mitochondrial ND4 Mutations in 1281 Han Chinese Subjects With Leber's Hereditary Optic Neuropathy. Invest Ophthalmol Vis Sci 2015; 56:4778-88. [PMID: 26218905].

24. Riordan-Eva P, Harding AE. Leber's hereditary optic neuropathy: the clinical relevance of different mitochondrial DNA mutations. J Med Genet 1995; 32:81-7. [PMID: 7760326].

25. Newman NJ, Lott MT, Wallace DC. The clinical characteristics of pedigrees of Leber's hereditary optic neuropathy with the 11778 mutation. Am J Ophthalmol 1991; 111:750-62. [PMID: 2039048].

26. Johns DR, Heher KL, Miller NR, Smith KH. Leber's hereditary optic neuropathy. Clinical manifestations of the 14484 mutation. Arch Ophthalmol 1993; 111:495-8. [PMID: 8470982].

27. Johns DR, Smith KH, Miller NR. Leber's hereditary optic neuropathy. Clinical manifestations of the 3460 mutation. Arch Ophthalmol 1992; 110:1577-81. [PMID: 1444915].

28. Marotta R, Chin J, Quigley A, Katsabanis S, Kapsa R, Byrne E, Collins S. Diagnostic screening of mitochondrial DNA mutations in Australian adults 1990–2001. Intern Med J 2004; 34:10-9. [PMID: 14748908].

29. Eustace Ryan S, Ryan F, Barton D, O'Dwyer V, Neylan D. Development and validation of a novel PCR-RFLP based method for the detection of 3 primary mitochondrial mutations in Leber's hereditary optic neuropathy patients. Eye Vis (Lond) 2015; 2:18-.

30. Bi R, Zhang AM, Yu D, Chen D, Yao YG. Screening the three LHON primary mutations in the general Chinese population by using an optimized multiplex allele-specific PCR. Clin Chim Acta 2010; 411:1671-4. .

31. Wang JY, Gu YS, Wang J, Tong Y, Wang Y, Shao JB, Qi M. MGB probe assay for rapid detection of mtDNA11778 mutation in the Chinese LHON patients by real-time PCR. J Zhejiang Univ Sci B 2008; 9:610-5. [PMID: 18763310].

32. White HE, Durston VJ, Seller A, Fratter C, Harvey JF, Cross NC. Accurate detection and quantitation of heteroplasmic mitochondrial point mutations by pyrosequencing. Genet Test 2005; 9:190-9. [PMID: 16225398].

33. Guo Y, Li J, Li CI, Shyr Y, Samuels DC. MitoSeek: extracting mitochondria information and performing high-throughput mitochondria sequencing analysis. Bioinformatics 2013; 29:1210-1. [PMID: 23471301].

34. Dwight Z, Palais R, Wittwer CT. uMELT: prediction of high-resolution melting curves and dynamic melting profiles of PCR products in a rich web application. Bioinformatics 2011; 27:1019-20. [PMID: 21300699].

35. Lesnik EA, Freier SM. Relative thermodynamic stability of DNA, RNA, and DNA:RNA hybrid duplexes: relationship with base composition and structure. Biochemistry 1995; 34:10807-15. [PMID: 7662660].